

ARE THE RED HALOS OF GALAXIES MADE OF LOW-MASS STARS? CONSTRAINTS FROM SUBDWARF STAR COUNTS IN THE MILKY WAY HALO

ERIK ZACKRISSON^{1,2,3*}, & CHRIS FLYNN¹

Draft version October 30, 2018

ABSTRACT

Surface photometry detections of red and exceedingly faint halos around galaxies have resurrected the old question of whether some non-negligible fraction of the missing baryons of the Universe could be hiding in the form of faint, hydrogen-burning stars. The optical/near-infrared colours of these red halos have proved very difficult to reconcile with any normal type of stellar population, but can in principle be explained by advocating a bottom-heavy stellar initial mass function. This implies a high stellar mass-to-light ratio and hence a substantial baryonic mass locked up in such halos. Here, we explore the constraints imposed by current observations of ordinary stellar halo subdwarfs on a putative red halo of low-mass stars around the Milky Way. Assuming structural parameters similar to those of the red halo recently detected in stacked images of external disk galaxies, we find that a smooth halo component with a bottom-heavy initial mass function is completely ruled out by current star count data for the Milky Way. All viable smooth red halo models with a density slope even remotely similar to that of the stacked halo moreover contain far too little mass to have any bearing on the missing-baryon problem. However, we note that these constraints can be sidestepped if the red halo stars are locked up in star clusters, and discuss potential observations of other nearby galaxies that may be able to put such scenarios to the test.

Subject headings: Galaxy: halo – galaxies: halos – galaxies: stellar content – dark matter – stars: subdwarfs

1. INTRODUCTION

The quest to unravel the nature of dark matter, estimated to make up around 90% of the total matter content (e.g. Komatsu et al. 2008), remains one of the most important tasks of modern cosmology. Dark matter appears to exist in at least two separate forms: one baryonic, and one non-baryonic. While the non-baryonic component is the dominant one, a substantial fraction of the baryons in the low-redshift Universe ($\approx 1/3$ – $2/3$; Fukugita 2004; Fukugita & Peebles 2004; Nicastro et al. 2005; Prochaska & Tumlinson 2008) are also at large.

These missing baryons could in principle be hiding in a variety of different forms: as faint/failed stars or stellar remnants (so-called Massive Astrophysical Compact Halo Objects or MACHOs; Griest 1991), as cold gas clouds (Pfenniger et al. 1994; Pfenniger & Combes 1994), as a warm/hot intergalactic medium (Cen & Ostriker 1999; Davé et al. 2001) or as hot gaseous halos around galaxies (Maller & Bullock 2004; Fukugita & Peebles 2006; Sommer-Larsen 2006). While current simulations seem to favour the latter two alternatives as the main reservoirs, observations are still unable to confirm this hypothesis (see Bregman 2007, for a review).

The old idea of baryonic dark matter in the form of faint, low-mass stars has recently gained new momentum through surface photometry detections of very red and exceedingly faint structures – “red halos” – around galaxies of different types. The history of this topic goes

back to the mid-90s, when deep optical and near-IR images indicated the presence of a faint halo around the edge-on disk galaxy NGC 5907 (e.g. Sackett et al. 1994; Lequeux et al. 1996; Rudy et al. 1997; James & Casali 1998). The colours of this structure were much too red to be reconciled with any normal type of stellar population, and indicative of a halo population with an abnormally high fraction of low-mass stars. At around the same time, Molinari et al. (1994) also announced the detection of a red halo around the cD galaxy at the centre of the galaxy cluster Abell 3284. Skepticism grew with the discovery of what appeared to be the remnants of a disrupted dwarf galaxy close to NGC 5907 (Shang et al. 1998), leading to suggestions that this feature, in combination with other effects, could have resulted in a spurious halo detection (Zheng et al. 1999). While follow-up observations with the Hubble Space Telescope (HST) took some of the edge out of this criticism (Zepf et al. 2000), the field fell into disrepute. Deeper images have later revealed a wealth of tidal streams in the halo of NGC 5907 (Martínez-Delgado et al. 2008), but this does not by itself explain the red excess originally detected.

The red halos would not die quietly though, and new reports started to surface a few years later. First, Bergvall & Östlin (2002) and Bergvall et al. (2005) presented deep optical/near-IR images of faint and abnormally red structures around blue compact galaxies. Zibetti, White, & Brinkmann (2004) then stacked images of 1047 edge-on disk galaxies from the Sloan Digital Sky Survey (SDSS) and detected a halo population with a strong red excess and optical colours curiously similar to those previously derived for NGC 5907 – again very difficult to reconcile with standard halo populations. The halo detected around an edge-on disk galaxy at redshift $z = 0.322$ in the Hubble Ultra Deep Field shows similarly

* E-mail: ez@astro.su.se

¹ Tuorla Observatory, Department of Physics and Astronomy, University of Turku, Väisäläntie 20, FI-21500 Piikkiö, Finland

² Stockholm Observatory, AlbaNova University Center, 106 91 Stockholm, Sweden

³ Department of Astronomy and Space Physics, Box 515, 751 20 Uppsala, Sweden

red colours (Zibetti & Ferguson 2004), and Tamm et al. (2007) argue that even the halo of Andromeda displays a pronounced red excess.

Zackrisson et al. (2006) analyzed the colours of some of these new detections and found that the halos of both blue compact galaxies and stacked edge-on disks could be explained by a stellar population with a very bottom-heavy initial mass function ($dN/dM \propto M^{-\alpha}$ with $\alpha \approx 4.50$). The high mass-to-light ratio of such a population makes it a potential reservoir for at least part of the baryons missing from current inventories. While the stellar initial mass function (IMF) is often assumed to be universal, recent observational studies suggest that it may vary both as a function of environment (Hoversten & Glazebrook 2008), and as a function of cosmic time (van Dokkum 2008). Corroborating evidence for an IMF as extreme as that advocated by Zackrisson et al. (2006) also comes from star counts in the field population of the LMC, where a slope of $\alpha \approx 5-6$ was derived for masses $\geq 1 M_{\odot}$ (Massey 2002; Gouliermis et al. 2006).

Taking the red halo detections at face value, one may ask whether the Milky Way itself could be surrounded by a hitherto undetected red halo of low-mass, hydrogen-burning stars, with photometric properties similar to the halo detected around stacked edge-on disks. The known baryonic components (thin disc, thick disk, bulge and standard stellar halo) of the Milky Way contribute around $5-6 \times 10^{10} M_{\odot}$ (e.g. Sommer-Larsen & Dolgov 2001; Klypin et al. 2002; Flynn et al. 2006) to the Milky Way's virial mass of $\approx 1 \times 10^{12} M_{\odot}$ (Klypin et al. 2002). A cosmic baryon fraction of $\Omega_{\text{baryons}}/\Omega_{\text{M}} \approx 0.17$ (Komatsu et al. 2008), combined with the theoretical prediction that the baryon fraction should be $\approx 90\%$ of the cosmic average for a Milky Way-sized halo (Crain et al. 2007), on the other hand suggests the presence of some $\approx 1.5 \times 10^{11} M_{\odot}$ of baryonic material within its virial radius, leaving at least 60% of its baryons to be found.

Low-mass stars would in principle be detectable through microlensing effects, and such putative MACHOs may already have been discovered in the halos of both the Milky Way and M31 (e.g. Alcock et al. 2000; Calchi Novati et al. 2005; Riffeser et al. 2008). Their masses ($0.1-1 M_{\odot}$) and inferred contribution to the mass of the dark matter of galaxies ($\approx 20\%$) are, however, very difficult to reconcile with any kind of stellar MACHO candidate (e.g. Freese 2000). This result, coupled to the fact that competing teams have failed to confirm these detections (Tisserand et al. 2007; de Jong et al. 2006) have led to the suspicion that the observations must have been misinterpreted (e.g. Belokurov et al. 2004) or that the compact objects detected through this technique may be of non-baryonic origin (e.g. primordial black holes, mirror matter objects, preon stars or scalar dark matter miniclusters – see Zackrisson & Riehm 2007 for a more thorough discussion).

If some of the missing baryons of the Milky Way are locked up in the form of hydrogen-burning stars in a red halo, such a structure must also have evaded the faint star counts aimed to constrain the luminosity function of halo subdwarfs (e.g. Gould et al. 1998; Gould 2003; Digby et al. 2003; Brandner 2005), since no significant excess of low-mass stars has yet been detected with this method. In fact, direct observations of this kind are expected to impose much stronger constraints on main sequence stars

in the halo than what current microlensing surveys can achieve.

In this paper, we explore to what extent a smooth red halo of low-mass stars similar to that detected by Zibetti et al. (2004) might already be ruled out by these observations of halo subdwarfs in the Milky Way. In section 2, we describe the observational data used. Section 3 outlines the method used to test red halo models against these observations. The resulting constraints on red halo models are presented in section 4. Section 5 discusses the robustness of these constraints and section 6 summarizes our findings.

2. OBSERVATIONAL DATA

2.1. Surface photometry

Using stacked SDSS images of 1047 edge-on galaxies, Zibetti et al. (2004, hereafter Z04) derived the colours of a diffuse halo in a wedge-shaped region located at a projected distance of $R_{\text{proj}} = 2 \times r_{\text{exp}}$ from the centre of the stacked disk, where r_{exp} corresponds to the exponential scale length of the disk. While the $g-r$ colour of this region ($g-r = 0.65 \pm 0.1$) is similar to those of old stellar populations like globular clusters or elliptical galaxies, $r-i$ is anomalously red ($r-i = 0.60 \pm 0.1$) and difficult to reconcile with any known type of stellar population. These colours can, however, be explained in the framework of a stellar population with an IMF slope of $\alpha = 4.50$ (Zackrisson et al. 2006), i.e. a stellar halo overly abundant in low-mass stars. One the other hand, the wavelength-dependence of the far wings of the point-spread function (PSF) may introduce spurious colours in the outskirts of extended objects (e.g. Michard 2002; Sirianni et al. 2005). Recently, de Jong (2008) has argued that Z04 may have underestimated the effects of the SDSS PSF, and that the reported $r-i$ halo colour therefore suffers from artificial reddening due to scattered light. At the current time, it is very difficult to assess whether this accounts for all of the red excess, or just some part thereof. With this in mind, the IMF slope of $\alpha = 4.50$ derived by Zackrisson et al. (2006) is likely to represent an upper limit, barring systematic uncertainties in the fit due to lingering problems with current models for low-mass stars (e.g. Casagrande et al. 2008). In what follows, we will use the i -band data of Z04, but allow for the possibility that both the overall surface brightness level of the halo and the colour may have been overestimated.

When comparing this average halo to the Milky Way, we have adopted a scale length for the Milky Way's disk of $r_{\text{exp}} = 2.5$ kpc, in agreement with recent estimates based on both optical and near-infrared data (Gardner et al. 2008). The measured i -band surface brightness level of the wedge in the stacked frame is $\mu_{\text{red}, i} \approx 26.7$ mag arcsec $^{-2}$, but we also explore the consequences of putative red halos with surface brightness levels both brighter and fainter than this. There are several reasons for this strategy. Firstly, part of the light measured at this distance is likely to come from the disk and the far wings of the SDSS PSF, implying that the red halo should be somewhat *fainter* at this distance than suggested by the surface brightness level actually measured. Secondly, the analysis presented by Z04 indicates that the surface brightness of the halo scales with the lumi-

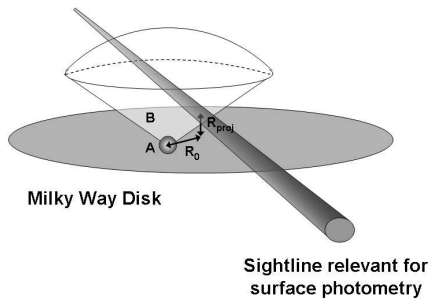


FIG. 1.— Schematic illustration of the relevant data situation. The volumes probed by the subdwarf observations of Digby et al. (2003) and Gould et al. (1998) are indicated by the gray sphere marked A and the cone marked B, respectively. R_0 represents the distance from the Galactic centre to the position of the Sun. The sightline along which the red halo colours have been measured through surface photometry around stacked SDSS disks is indicated by the gray cylinder, located at a projected distance of R_{proj} above the plane of the disk.

osity of the disk, which would suggest a red halo *brighter* than $\mu_{\text{red}, i} \approx 26.7$ at $R_{\text{proj}} = 2 \times r_{\text{exp}}$ for a relatively luminous galaxy like the Milky Way. On the other hand, it is not clear what the distribution of red halo properties within the stacked sample is, and individual differences between galaxies may possibly compensate for such a trend. Here, we therefore consider the possibility that a hypothetical red halo surrounding the Milky Way could be substantially different than the cosmic average as derived by Z04.

While Z04 derive a halo flattening of $q \approx 0.6$ and a density profile with power-law slope $\beta \approx 3$ for the i -band, we here explore the consequences of red halos with $q = 0.5\text{--}1.5$ and power $\beta = 0\text{--}10$. This very generous range of parameter values ensure that the constraints derived are conservative, in the sense that they allow any hypothetical red halo maximal leverage.

2.2. Star counts

Subdwarfs are main sequence stars in the mass range $\approx 0.08\text{--}1 M_{\odot}$ that because of their low metallicities have lower V -band luminosities than disk stars of the same colour. These objects make up the bulk of stars in the hitherto detected stellar halo of the Milky Way, and have been used in numerous studies to constrain the characteristics of this structure. Since adopting a bottom-heavy IMF of the Zackrisson et al. (2006) type would boost the fraction of subdwarfs in a population, it makes sense to use the observed number densities of these objects to constrain such scenarios.

Large samples of halo subdwarfs can be collected using two different techniques: proper-motion selection and colour-magnitude selection in deep fields.

The first method exploits the high heliocentric velocities statistically expected from stars belonging to the halo and selects candidate halo stars by imposing a minimum proper motion limit on the sample (e.g. Gould 2003; Digby et al. 2003). A kinematical model is then used to correct the resulting statistics for incompleteness

and contamination by thin and thick disk stars. This method is currently limited to halo stars within a few kpc from the position of the Sun.

The second method is based on identification of stars in long exposures (“deep fields”) of the sky at high Galactic latitudes (Gould et al. 1998; Brandner 2005) and the use of colour-magnitude criteria to reject objects in the disk. While this technique probes subdwarfs at much fainter magnitude limits (and thereby larger distances) than the former, the selection criteria prevent it from probing subdwarfs within a few kpc of the Sun.

The volumes probed by these two methods are complementary, with almost no overlap. Curiously enough, the scaling of the luminosity function of halo subdwarfs derived by these two techniques differ somewhat (by a factor of 2–3; see Digby et al. 2003, for a comparison). The exact reason for this discrepancy is not well-understood, but could possibly be due to a difference in the characteristics of the inner and outer halo. Indeed, Carollo et al. (2007) recently found strong evidence for two separate structural components in the Galactic halo, with the inner halo being substantially more flattened than the outer.

Here we make no attempt to reconcile the measurements resulting from these different techniques. Instead, we assume that the subdwarf luminosity functions and the halo parameters derived by the two techniques are correct in the mutually exclusive volumes for which they are relevant. In what follows, we therefore consider two sets of constraints, A and B, based on the proper-motion samples of by Digby et al. (2003) and the deep-field samples of Gould et al. (1998), respectively. Even though there are many large studies based on the first technique, the differences between these and those of Digby et al. (2003) are minor and will not have any significant impact on the current study. While there are slight differences between the assumptions made in Gould et al. (1998) and Digby et al. (2003) about the functional form of density profile of the stellar halo, both studies are able to produce good fits to the number of subdwarfs observed in the volumes probed, and this is what matters for the current study.

Digby et al. (2003) assume a density profile for the stellar halo of the form⁵:

$$n_{\text{A}}(x, y, z) = n_{\text{A}, \odot} \left(\frac{x^2 + y^2 + (z/q)^2 + R_0^2}{R_0^2 + R_c^2} \right)^{-\beta/2}, \quad (1)$$

where x, y, z are galactocentric coordinates. n_{\odot} is the number density of subdwarfs in the vicinity of the Sun, q is the halo flattening parameter, R_0 is the distance from the Sun to the centre of the Milky Way (throughout this paper assumed to be 8.0 kpc), R_c is a core radius (assumed to be $R_c = 1.0$ kpc) and β is the exponent of the density power-law. While Digby et al. (2003) are unable to impose useful constraints on q , they find a best-fitting $\beta = 3.15$ and adopt $q = 0.55$ in their plots. In what follows, these values will be adopted by us as well.

Gould et al. (1998) instead assume that the subdwarfs of the stellar halo are distributed according to a density

⁵ Here, we have corrected an obvious misprint in Digby et al. (2003), related to the definition of β .

profile of the form:

$$n_{\text{B}}(x, y, z) = n_{\text{B},\odot} \left(\frac{x^2 + y^2 + (z/q)^2}{R_0^2} \right)^{-\beta/2}. \quad (2)$$

where x, y, z are galactocentric coordinates. With this assumption, they derive best fitting values of $\beta = 3.13$ and $q = 0.82$.

To derive $n_{\text{A},\odot}$ and $n_{\text{B},\odot}$, we need to adopt a luminosity range for subdwarfs. For simplicity, we consider all main sequence stars that fall in the luminosity range probed by *both* Digby et al. (2003) and Gould et al. (1998) to be subdwarfs, i.e. objects with V -band luminosities $7.5 \lesssim M_V \lesssim 12.4$. This then implies $n_{\text{A},\odot} \approx 1.7 \times 10^5 \text{ kpc}^{-3}$ and $n_{\text{B},\odot} \approx 6.4 \times 10^4 \text{ kpc}^{-3}$.

3. STAR COUNTS CONFRONT SURFACE PHOTOMETRY

Here we use the best-fitting halo parameters derived by Digby et al. (2003) and Gould et al. (1998) to compute the mean number densities of subdwarfs $\overline{n_{\text{A}}}$ and $\overline{n_{\text{B}}}$ within the relevant volumes V_{A} and V_{B} :

$$\overline{n_{\text{A/B}}} = \frac{1}{V_{\text{A/B}}} \int n_{\text{A/B}}(x, y, z) dV_{\text{A/B}}. \quad (3)$$

Any additional, smooth halo population that involves higher subdwarf densities than $\overline{n_{\text{A}}}$ or $\overline{n_{\text{B}}}$ in these volumes should already have been detected in either the Digby et al. (2003) or Gould et al. (1998) surveys and can therefore be ruled out. By simply checking $\overline{n_{\text{A}}}$ and $\overline{n_{\text{B}}}$ against the predictions of various red halo models, we can therefore place conservative – yet very strong – constraints on any hitherto undetected, smooth red halo of low-mass stars around the Milky Way.

The volumes A and B considered relevant for the studies by Digby et al. (2003) and Gould et al. (1998) are illustrated in Fig. 1. For simplicity, we take the volume covered by Digby et al. (2003) to be a sphere with radius 2.8 kpc centered on the position of the Sun. In the case of Gould et al. (1998), the actual volumes probed correspond to an ensemble of many very narrow cones of different length (given by the flux limits of the HST fields used), with their tips removed to avoid contamination from stars belonging to the disk. Here, we approximate these volumes by a single, wide cone with opening angle 60° and height 40 kpc, with the tip (within 2.3 kpc of the plane) removed. In Fig. 1, we have only depicted one cone, whereas in reality, stars were selected from both directions away from the Milky Way disk. Since we are only considering halo models that are symmetric with respect to the disk, this has no impact on our results. Using $V_{\text{A}} \approx 92 \text{ kpc}^3$ and $V_{\text{B}} \approx 1.8 \times 10^4 \text{ kpc}^3$, and the density profiles described in section 2.2, we find $\overline{n_{\text{A}}} \approx 1.7 \times 10^5 \text{ subdwarfs kpc}^{-3}$ and $\overline{n_{\text{B}}} \approx 1.2 \times 10^3 \text{ subdwarfs kpc}^{-3}$.

Also plotted in Fig. 1 is the line of sight (for simplicity depicted as a cylinder) for which surface photometry indicates anomalously red colours in the stacked halo data of Z04. This region is located at a projected distance of $R_{\text{proj}} = 2 \times r_{\text{exp}}$ from the midplane of the disk, which – when rescaled to a galaxy with the dimensions adopted for the Milky Way – corresponds to $R_{\text{proj}} = 5 \text{ kpc}$. This sightline may or may not directly intersect the volume B probed by deep-field star counts, depending on the (undetermined) orientation of the Sun with respect to the surface brightness sightline. However, in the

axisymmetric halo models considered here, this is of no consequence. The important point is instead that, because of the projected nature of the surface photometry data, contributions from the light measured along the depicted sightline can come from regions outside (i.e. in front of, or behind) the Gould et al. (1998) cone. Therefore, the available star counts do not necessarily dictate what would be observed along the surface photometry sightline, although they do set a lower limit on the total surface brightness.

3.1. Rejection criteria

When testing red halo models against the observational constraints, we assume that the red halo is smooth and can be described by a density profile of the form:

$$n_{\text{red}}(x, y, z) = n_{\text{red},\odot} \left(\frac{x^2 + y^2 + (z/q_{\text{red}})^2}{R_0^2} \right)^{-\beta_{\text{red}}/2} \quad (4)$$

where x, y, z are Galactocentric coordinates. n_{red} is the number density of subdwarfs, q_{red} the flattening parameter for the red halo and β_{red} the exponent of the red halo density power-law. This matches the assumptions used in the work of Gould et al. (1998).

For each combination of red halo model parameters considered, we calculate the expected mean number densities of red halo subdwarfs in volumes A and B:

$$\overline{n_{\text{red, A/B}}} = \frac{1}{V_{\text{A/B}}} \int n_{\text{red}}(x, y, z) dV_{\text{A/B}}. \quad (5)$$

All red halo models that give either $\overline{n_{\text{red, A}}} > \overline{n_{\text{A}}}$ or $\overline{n_{\text{red, B}}} > \overline{n_{\text{B}}}$ are then considered rejected. Given the red halo density profile parameters q_{red} and β_{red} , the normalization parameter $n_{\text{red},\odot}$ is computed from the requirement that surface brightness of the red halo, at a projected distance from the Milky Way disk of $2 \times r_{\text{exp}}$ is equal to the observed $I_{\text{red, }i}$, i.e. $\mu_{\text{red, }i}$ converted from mag arcsec^{-2} to $L_{\text{AB}} \text{ kpc}^{-2}$:

$$I_{\text{red, }i} = \frac{2n_{\text{red},\odot}}{N_{\text{sub}}/L_i} \int_0^{y_{\text{max}}} \left(\frac{y^2 + \left(\frac{2r_{\text{exp}}}{q_{\text{red}}}\right)^2}{R_0^2} \right)^{-\frac{\beta_{\text{red}}}{2}} dy. \quad (6)$$

Here N_{sub}/L_i describes the number of subdwarfs per luminosity (in units of $L_{\text{AB},i}$, i.e. the i -band luminosity of the flat-spectrum source used to define the zero point of the SDSS AB system) in the red halo population. The upper integration limit is given by $y_{\text{max}} = \sqrt{r_{\text{max}}^2 - 4r_{\text{exp}}^2}$, where r_{max} is the outer truncation radius of the red halo. To allow any putative red halo maximum leverage, we set r_{max} equal to the virial radius of the dark matter halo, which we here take to be 258 kpc (Klypin et al. 2002).

This leads to four free parameters for the red halo model: q_{red} , β_{red} , N_{sub}/L_i and $\mu_{\text{red, }i}$.

For red halo models that remain viable after constraints A and B have been imposed, we compute the mass contained in such structures using:

$$M_{\text{red}} = \left(\frac{M}{N_{\text{sub}}} \right) \int_0^{2\pi} \int_0^\pi \int_{r_{\text{min}}}^{r_{\text{max}}} n(r, \theta, \phi) r^2 \sin(\theta) dr d\theta d\phi, \quad (7)$$

TABLE 1
 N_{sub}/L_i AND M/N_{sub} AS A
 FUNCTION OF IMF SLOPE α .

α	N_{sub}/L_i	M/N_{sub}
0.75/2.35 ^a	67	1.7
2.35	300	0.59
3.00	650	0.60
3.50	1100	0.70
4.00	1800	0.86
4.50	2400	1.1
5.00	2700	1.4

^aThis entry represents the two-component power-law IMF considered representative for the standard stellar halo of the Milky Way.

where M/N_{sub} represents the ratio of total mass of the red halo stellar population (in the 0.08–120 M_{\odot} mass range) to the number of such stars considered subdwarfs, and $n(r, \theta, \phi)$ is simply equation (4) converted into spherical coordinates. Since we have assumed a core-free, power-law density for the red halo (eq. 4), a non-zero lower radial integration limit r_{min} is required to prevent M_{red} from diverging for $\beta_{\text{red}} > 0$. Here, we have adopted $r_{\text{min}} = 1$ kpc. Allowing a smaller r_{min} would only have a significant impact on M_{red} for very steep density profiles (i.e. profiles with high β_{red}), since these attain very high central densities. However, such populations are of little interest for the missing-baryon problem, since models that attempt to hide a substantial baryonic mass in the form of stars within ~ 1 kpc from the Milky Way centre are subject to very strong constraints by microlensing observations towards the bulge (Calchi Novati et al. 2008).

3.2. Spectral synthesis

To determine reasonable values for the parameter N_{sub}/L_i in equation (6), spectral synthesis modelling is required. The constraints presented in Section 4 are based on the assumption that the red halo has an age of 10 Gyr, a metallicity of $Z = 0.001$, and a power-law IMF with exponent α ($dN/dM \propto M^{-\alpha}$) throughout the mass range 0.08–120 M_{\odot} . The star formation rate (SFR) is assumed to have been exponentially declining over cosmological time scales ($\text{SFR} \propto \exp(-t/\tau)$), with $\tau = 1$ Gyr (suitable for an early-type system). Since the resulting constraints are somewhat sensitive to the parameter values adopted, the effects of relaxing these assumptions are carefully explored in Section 5.

To derive N_{sub}/L_i , we also need to identify the subset of stars in the red halo population that qualify as subdwarfs. The luminosity criteria described in section 2.2 convert into a stellar mass range of $0.15 \lesssim M(M_{\odot}) \lesssim 0.7$ (e.g. Marigo et al. 2007). The number of subdwarfs N_{sub} within a population can then straightforwardly be derived from the IMF, whereas the integrated i -band luminosity and the stellar population mass M can be derived using a spectral synthesis code. Here, we use the population synthesis model PEGASE.2 (Fioc & Rocca-Volmerange 1999) to derive these quantities.

The constraints on red halo models derived in section 4 will be computed for the N_{sub}/L_i values (in units of

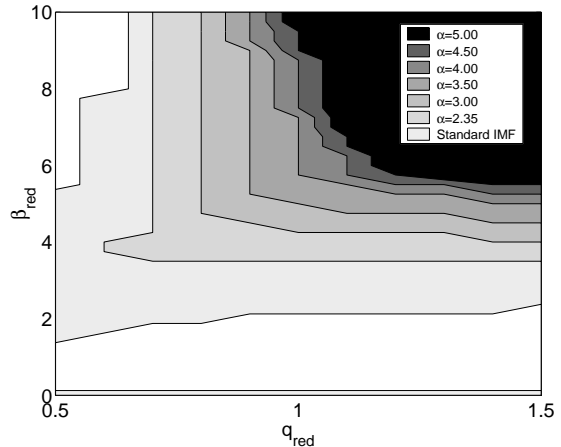


FIG. 2.— The regions in the $(\beta_{\text{red}}, q_{\text{red}})$ parameter space allowed for different red halo IMFs (shades of gray) in the case of $\mu_{\text{red}, i} = 26.7$ mag arcsec⁻². The constraints are based on the Digby et al. (2003) and Gould et al. (1998) surveys combined – i.e. red halos are considered rejected if either $\bar{n}_{\text{red}, A} > \bar{n}_A$ (conflict with Digby et al. 2003) or $\bar{n}_{\text{red}, B} > \bar{n}_B$ (conflict with Gould et al. 1998). The “Standard IMF” refers to the broken power-law IMF considered representative of the hitherto detected stellar halo of the Milky Way. Darker areas (corresponding to more bottom-heavy IMFs) are here plotted on top of brighter ones, so that the region marked by the darkest shade of gray indicates the boundaries inside which halos of *any* IMF (ranging from the standard IMF to the $\alpha = 5.00$ IMF) are allowed to lie. Halo models with the standard IMF are on the other hand only constrained to lie within the union of all the differently shaded areas. The $(q_{\text{red}}, \beta_{\text{red}})$ constraints on halo models with less extreme IMFs (lighter shades of gray) are consequently much weaker than those of the most bottom-heavy ones (darker shades of gray). White regions represent regions of the parameter space where no red halo models are allowed.

dwarfs $L_{\text{AB}, i}^{-1}$) listed in Table. 1. These correspond to the predictions for IMF slopes $\alpha = 2.35$ (i.e. the Salpeter IMF), 3.00, 3.50, 4.00, 4.50 (the value favoured by Zakrisson et al. 2006) and 5.00. For comparison, we also list N_{sub}/L_i for an IMF that more closely resembles that of the hitherto detected stellar halo: a broken power-law IMF with $\alpha = 0.75$ in the 0.08–0.7 M_{\odot} mass range and $\alpha = 2.35$ for 0.7–120 M_{\odot} . This choice (labeled 0.75/2.35 in Table 1) is in fair agreement with the mass function derived by Gould et al. (1998), and produces results similar to other parameterizations of the halo IMF (e.g. Chabrier 2003). The M/N_{sub} ratios, required to compute the stellar population masses of viable red halo models using equation (7), are also listed for these IMFs.

These IMFs cover the range from perfectly normal to extremely bottom-heavy, and therefore account for the possibility that the $r - i$ colour (the primary reason for advocating a steep IMF slope) reported by Z04 may have been artificially reddened by PSF effects (de Jong 2008).

4. CONSTRAINTS ON RED HALO MODELS

By simply adopting the best-fitting structural parameters derived by Z04 ($q_{\text{red}} \approx 0.6$, $\beta_{\text{red}} \approx 3$) and assuming a bottom-heavy IMF population with $\alpha = 4.50$ for the red halo colours, we would arrive at a red halo mass of $M_{\text{red}} \approx 2 \times 10^{10} M_{\odot}$. While this is in the right ballpark for accounting for a significant fraction of the missing baryons in the Milky Way, this parameter combination – along with all similar ones – are completely ruled out by the star counts. This is demonstrated in Fig. 2,

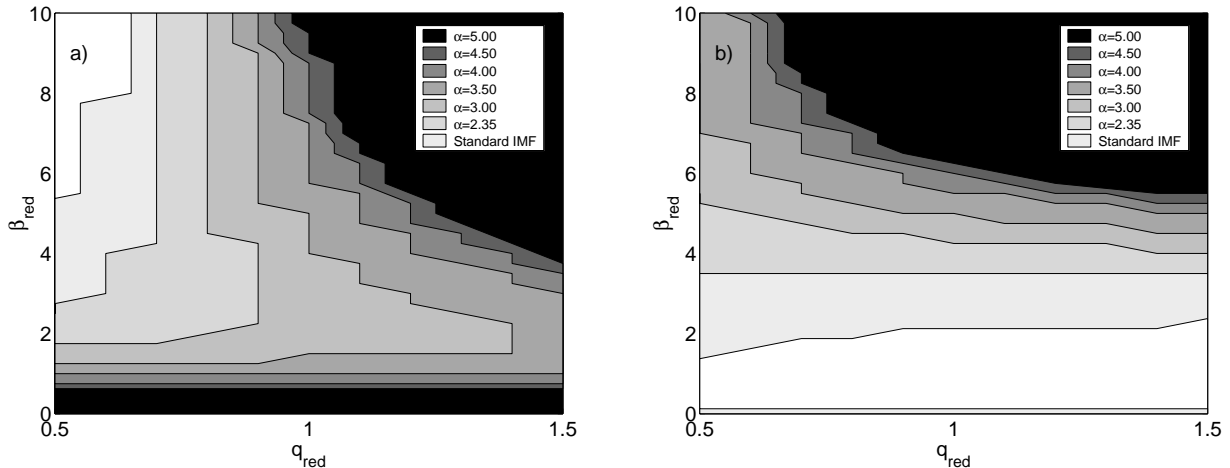


FIG. 3.— Same as Fig. 2, but showing the regions of the $(\beta_{\text{red}}, q_{\text{red}})$ red halo parameter space allowed by the data sets of (a) Digby et al. (2003) and (b) Gould et al. (1998), separately.

where we apply the combined constraints imposed by the Digby et al. (2003) and Gould et al. (1998) surveys to red halo models with parameters in the range $\beta_{\text{red}} = 0\text{--}10$ (where $\beta_{\text{red}} = 0$ corresponds to a constant-density halo) and $q_{\text{red}} = 0.5\text{--}1.5$. For these constraints, we have assumed a scaling given by a halo surface brightness level of $\mu_{\text{red}, i} = 26.7 \text{ mag arcsec}^{-2}$ (in direct correspondence to the stacked halo by Z04).

A wide range of different model parameters are allowed in the case of the standard halo IMF (lightest shade of gray), including the $\beta = 3\text{--}3.5$, $q = 0.5\text{--}1.0$ range in which the hitherto detected stellar halo is known to lie. Of course, this IMF cannot account for the anomalously red colours of the Z04 halo, and the mass of such structure is only about $1 \times 10^9 M_{\odot}$, in fair agreement with estimated total mass of the ordinary stellar halo of the Milky Way (e.g. Bell et al. 2008).

As the IMF becomes more bottom-heavy, the allowed region of the parameter space is progressively pushed into the upper right corner of this diagram. The most bottom-heavy IMFs considered (darkest shades of gray) are only allowed at $q_{\text{red}} > 1$ (i.e. halos elongated in the polar direction) and $\beta_{\text{red}} > 5$ (i.e. halos where the density drops much faster as a function of distance from the centre than the standard halo with $\beta \approx 3$). Because of their high central densities, such models more closely resemble elongated bulges than normal halos.

The range of density profile slopes ($\beta_{\text{red}} = 2.5\text{--}3.5$) and flattenings ($q_{\text{red}} = 0.5\text{--}0.7$) favoured by Z04 are *completely ruled out* for the Milky Way in the case of the more bottom-heavy IMF slopes. While there are indeed red halo models ($\beta_{\text{red}} > 5$) with very bottom-heavy IMFs that would be able to explain the i -band surface brightness while evading the constraints set by current star counts, *the mass contained in such structures is very low*. In the case of $\alpha = 4.0\text{--}5.0$ (i.e. an IMF similar to that advocated by Zackrisson et al. 2006), the maximum red halo mass among the acceptable models is only $\approx 5 \times 10^8 M_{\odot}$, insufficient to be of any relevance for the missing-baryon problem.

Due to the different volumes probed by Digby et al. (2003) and Gould et al. (1998), these two data sets constrain slightly different regions of the $(\beta_{\text{red}}, q_{\text{red}})$ param-

eter space. This is demonstrated in Fig. 3, where the constraints imposed by Digby et al. (2003) and Gould et al. (1998) are plotted separately. While both sets of star counts are equally effective in ruling out the red halo models directly favoured by Z04 (i.e. $\beta_{\text{red}} = 2.5\text{--}3.5$ and $q_{\text{red}} = 0.5\text{--}0.7$), there are notable differences in the constraints imposed on more extreme models. Due to the smaller volume covered by Digby et al. (2003), their data are unable to rule out red halo models with close-to-constant densities (i.e. $\beta_{\text{red}} \approx 0$). While such models imply relatively few subdwarfs in the vicinity of the Sun, the fact that these densities are retained far into the halo – where the relevant volumes elements become huge – result in very large red halo masses ($\sim 10^{12} M_{\odot}$). Since the Gould et al. (1998) star counts are sensitive to subdwarfs at much greater distances from the Galactic centre, all $\beta_{\text{red}} \approx 0$ models are rejected in Fig. 3b. On the other hand, the position of the Digby et al. volume in the plane of the Milky Way imply that these star counts are more sensitive than the Gould et al. ones to red halo models which are flattened towards the disk (i.e. $q_{\text{red}} < 1.0$), and this is also the main contribution of Digby et al. to the combined constraints presented in Fig. 2.

4.1. Varying the brightness of the halo

In Fig. 4, we explore the maximum red halo mass allowed as a function of the adopted $\mu_{\text{red}, i}$ in the case of the $\alpha = 4.50$ IMF. Allowing any putative red halo around the Milky Way an i -band surface brightness level brighter than $\mu_{\text{red}, i} = 26.7 \text{ mag arcsec}^{-2}$ has the effect of pushing the allowed parameter space for the bottom-heavy models farther into the upper right corner of Fig. 2, i.e. to higher β_{red} and q_{red} . As a result, the largest red halo masses among models with IMF slopes of $\alpha = 4.0\text{--}5.0$ also become somewhat smaller than those in the case of $\mu_{\text{red}, i} = 26.7 \text{ mag arcsec}^{-2}$. This means that, if the red halo component is brighter in the Milky Way than in the stacked halo, the red excess can only be attributed to a stellar population with a bottom-heavy IMF if its density profile is much steeper than that of both the Galactic stellar halo and the stacked halo of external disk galaxies. Even if this were the case, the mass contained in

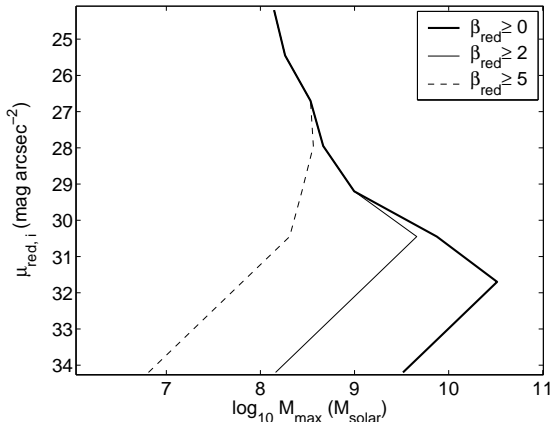


FIG. 4.— Maximum allowed red halo mass vs. the adopted surface brightness level $\mu_{\text{red},i}$ at r_{proj} for a halo population with IMF slope $\alpha = 4.50$ and different constraints on the slope of the red halo density profile: $\beta_{\text{red}} \geq 0$ (thick solid line), $\beta_{\text{red}} \geq 2$ (thin solid), and $\beta_{\text{red}} \geq 5$ (thin dashed).

this structure would be orders of magnitude below that required to have any relevance for the missing-baryon problem in the Milky Way.

As previously discussed, the i -band surface brightness of the halo may be contaminated by both a contribution from the disk and by the far wings of the PSF. Allowing a surface brightness level fainter than $\mu_i = 26.7$ mag arcsec $^{-2}$ increases the allowed parameter space for bottom-heavy IMFs. At $\mu_{\text{red},i} = 29.2$ mag arcsec $^{-2}$ (i.e. a factor of 10 fainter than the stacked halo), red halos with $\alpha = 4.50$ and structural parameters similar to the standard halo are allowed (e.g. $\beta_{\text{red}} = 3.5$, $q_{\text{red}} = 0.75$). However, since this has been made possible at the expense of a low overall density scaling, the maximum mass in such red halo models do not exceed $\sim 10^9 M_{\odot}$, which is insufficient to explain the missing baryons.

With a red halo as faint as $\mu_{\text{red},i} = 31.7$ mag arcsec $^{-2}$ (i.e. 100 times fainter than the stacked halo), the entire parameter space depicted in Fig. 2 becomes viable for all IMFs considered. As a result, red halos models with $\alpha = 4-5$ and masses in the range that would indeed be relevant for the missing-baryon problem (several times $10^{10} M_{\odot}$) evade the observational constraints considered here. However, as shown in Fig. 4 these high masses are produced exclusively by models with $2 > \beta_{\text{red}} \geq 0$. Density profile slopes like these are too shallow to be consistent with the slopes of $\beta_{\text{red}} = 2.5-3.5$ favoured by Z04. Since Z04 made no attempt to correct their surface brightness profiles for PSF effects, it is moreover likely that their estimate of β_{red} is an underestimate rather than an overestimate.

As is evident from Fig. 4, the maximum red halo mass reaches a peak at some $\mu_{\text{red},i}$ and then declines for fainter models, since the allowed region of the $(\beta_{\text{red}}, q_{\text{red}})$ plane initially grows as fainter halos are considered. However, once the entire plane becomes permitted, the only effect of going fainter is to lower the overall density scaling of the red halos, thereby giving smaller total masses.

Hence, while a red halo of low-mass stars can in principle evade the current constraints on halo subdwarfs and at the same time account for some non-negligible fraction of the missing baryons, this would require that *both* the

scaling and slope of its surface brightness profile would be very different from that of the halo seen around stacked external galaxies. Since the variance of red halo properties among disk galaxies cannot easily be assessed from the Z04 study, this possibility cannot be ruled out. However, advocating a solution of that type would relieve the stacked halo of all predictive power concerning the Milky Way, and we do not consider this possibility any further.

Allowing for the fact that the $r-i$ colour of the halo may have been overestimated (thereby implying a less extreme halo IMF) does not significantly alter these conclusions. All halo models with $\beta_{\text{red}} \geq 2$ that evade the star counts constraints have $M_{\text{max}} \leq 10^{10} M_{\odot}$ at all μ_i considered in Fig. 4, regardless of which of the IMFs in Table 1 we adopt.

5. DISCUSSION

Our results indicate that a smooth halo with a bottom-heavy IMF and structural parameters similar to those of the stacked halo is completely ruled out in the Milky Way by current star count data. A halo component with a bottom-heavy IMF would have to have an overall scaling or density profile that differs substantially from that of the stacked halo to remain viable. Moreover, all permitted smooth red halo models with a density slope *even remotely similar* to that of the stacked halo contain far too little mass to have any bearing on the missing-baryon problem in the Milky Way.

These conclusions are admittedly based on a large number of assumptions regarding the properties of the red halo. Since one can in principle consider many formation scenarios for a halo-like structure dominated by low-mass stars – for example in situ formation, population III stars, dynamical mass segregation (see Zackrisson et al. 2007, for a more details discussion) – the properties of the red halo population may be very different from those thus far adopted. Here, we therefore investigate the robustness of our conclusions in light of the most important assumptions made.

5.1. Age, star formation history and metallicity of the halo

In deriving the constraints presented in section 4, fixed N_{sub}/L_i ratios have been adopted for every IMF slope considered, based on the assumed age, prior star formation history and metallicity of the red halo. In reality, of course, we have but very poor constraints on these properties. For a halo population, one naively expects a relatively high age and a low metallicity, and we therefore restrict the discussion to ages $t \geq 1$ Gyr and metallicities $Z \leq 0.008$. In Fig. 5a and b, we demonstrate the dependence of N_{sub}/L_i on age and Z in the case of a stellar population with $\tau = 1$ Gyr. The N_{sub}/L_i ratio generally increases as a function of age.

However, for the more bottom-heavy IMFs (i.e. high IMF slope α), the age dependence is weak, and an age lower than the 10 Gyr assumed in section 4 would allow N_{sub}/L_i to be lowered by no more than $\approx 25\%$ (for $\alpha \geq 4$). Allowing a metallicity higher than the assumed value of $Z = 0.001$ would just increase N_{sub}/L_i and hence strengthen the constraints. A metallicity as low as $Z = 0.0001$ would decrease N_{sub}/L_i , but by no more than $\approx 30\%$. The maximum decrease is moreover attained at the highest ages, which means that this drop in N_{sub}/L_i

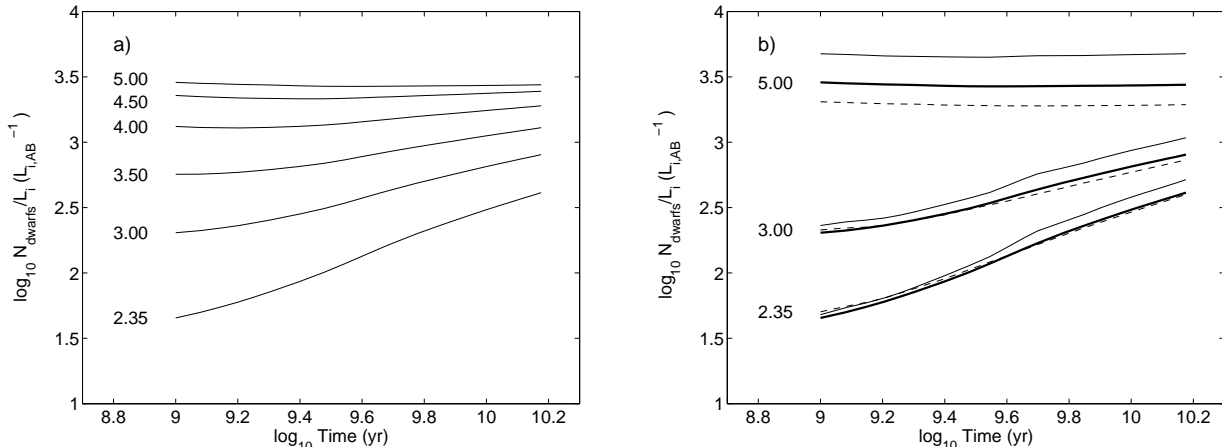


FIG. 5.— N_{sub}/L_i as a function of age for stellar populations with different IMF slopes α (indicated by labels). **a)** Populations with $Z = 0.001$ and $\tau = 1$ Gyr. **b)** Populations with $\tau = 1$ Gyr at metallicities of $Z = 0.0001$ (thin dashed), $Z = 0.001$ (thick solid) and $Z = 0.008$ (thin solid). To avoid cluttering, only a subset of IMF slopes are included.

does not add to the age effect – you cannot have both at the same time. Hence, the combined effect of age and metallicity is no more than $\approx 30\%$ for IMFs with $\alpha \geq 4$.

Alterations in the star formation history affect the N_{sub}/L_i ratio in a way that is very similar to age variations. The maximised N_{sub}/L_i are attained in the case of an instantaneous burst of star formation (i.e. a single-age population). While the perfectly coeval onset and quenching of star formation associated with this scenario seems unrealistic given the huge spatial scales involved in the halo, an instantaneous burst would just make the constraints on the red halo stronger. Allowing a more prolonged star formation history than the $\tau = 1$ Gyr adopted in section 4 on the other hand lowers N_{sub}/L_i . In the extreme case of having a star formation that increases as a function of time, the N_{sub}/L_i ratio stays almost constant at the value attained at the lowest ages. Hence, such scenarios do not provide the means for lowering N_{sub}/L_i more than the age effects already discussed.

In summary, N_{sub}/L_i for these alternative scenarios may be somewhat lower ($\approx 30\%$) than the values listed in Table 1 and used in the constraints presented in section 4. A detailed inspection of the entries in Table 1 reveals that this may shift the constraint levels by at most one level, in the sense that the constraints given for an IMF with slope α may be relaxed to mimic those for an IMF with a slope one step lower among those tested. As an example, changing the age from 10 to 1 Gyr for an $\alpha = 4.00$ model would lower N_{sub}/L_i from $N_{\text{sub}}/L_i \approx 1800$ to ≈ 1300 (see Fig. 5a), i.e. a decrease by $\approx 30\%$. This N_{sub}/L_i ratio is intermediate between those listed for $\alpha = 3.50$ and 4.00 . Hence, the relaxed constraints on the allowed structural parameters for a $\alpha = 4.00$ halo would fall between those of the $\alpha = 3.50$ and 4.00 contours in Fig. 2. This shift is too small to allow a halo population with $\alpha = 4.0$ – 5.0 into regions of the $(q_{\text{red}}, \beta_{\text{red}})$ parameter space where it would contribute significantly to the missing-baryon problem. Other spectral synthesis codes may produce slightly different values for N_{sub}/L_i , but the qualitative impact of such variations on the final constraints is easy to assess from Table 1 and Fig. 5.

Once the constraints on q_{red} and β_{red} have been deter-

mined, the mass of the viable red halo models are computed using equation (7), based on the M/N_{sub} ratio. This ratio also has a slight dependence on age and star formation history, but varies by no more than $\approx 30\%$ for IMFs with slopes $\alpha \geq 3$. The inferred red halo masses change insignificantly because of such effects.

Hence, we argue that our conclusions are robust with respect to the assumptions made about the age, metallicity and star formation history of the red halo.

5.2. Disk scale length

The constraints presented in section 4 have been derived using a scale length for the Milky Way of $r_{\text{exp}} = 2.5$ kpc. The effect of changing r_{exp} is to spatially shift the projected distance $r_{\text{proj}} = 2 \times r_{\text{exp}}$ between the plane of the disk and the region where the density scale of the red halo models are set by the assumed $\mu_{\text{red}, i}$. Adopting a smaller value of r_{exp} weakens the constraints imposed on red halo models by star counts in volumes A and B, whereas a larger r_{exp} would make the constraints stronger. Allowing $r_{\text{exp}} = 2.0$ kpc (at the lower limit of what is allowed by the constraints set by Juric et al. 2008) only allows an increase of the overall mass of red halos with IMFs with $\alpha = 4.0$ – 5.0 by a factor of ≈ 2 , which still places the red halo mass substantially below the range relevant for the missing-baryon problem in the Milky Way. Therefore, our conclusions seem very robust with respect to uncertainties in the scale length of the Milky Way disk.

5.3. Halo IMF

So far, we have only considered power-law IMFs with single-valued slopes α for the red halo population. In principle, far more complicated IMFs (e.g. broken power laws, lognormal IMFs, IMFs with mass spikes) could be considered. While this is not warranted given the large observational uncertainties associated with current red halo data, improved measurements may indeed require modifications of the assumed IMF. The revised constraints can be assessed by comparing N_{sub}/L_i and M/N_{sub} of populations with more complicated IMFs to the values listed in Table 1. However, as long as the

IMF is not tweaked to move a very large fraction of the overall population mass outside the stellar mass range to which the current subdwarf star counts are sensitive ($\approx 0.15 - 0.7 M_{\odot}$), the conclusions presented here will not be qualitatively altered.

5.4. Halo density profile

The constraints presented are based on the reasonable assumption that the volume density of red halo stars decreases monotonically with distance from the Galactic centre. Shells and tidal tails are sometimes seen in the outskirts of galaxies, and represent overdensities of matter that formally violate this assumption. If one entertained the notion that the abnormal colours of the red halo come from low-mass stars in a shell-like structure, then the constraints presented here can in principle be completely sidestepped by pushing the radius of this shell to distances outside the volume probed by the Gould et al. (1998) star counts (volume B in Fig. 1). However, while the density of such a structure can be chosen freely to correspond to the measured surface brightness level at any single projected radius, the decrease in surface brightness as a function of projected distance from the centre would be far slower than that reported by Z04.

So far, we have assumed the red halo density profile to be a single-valued power law, whereas more complicated density profiles can of course be considered. A broken power-law profile with a shallow slope (or a constant density core) close to the centre ($R_c < R_{\text{proj}}$) would result in constraints on the outer slope and flattening identical to those presented here, except that the overall red halo mass would become even lower than implied by current constraints for the allowed parameter combinations. The situation becomes more complicated if the power-law density profile changes slope inside (or even outside) the volumes A and B. However, a break of this type would be imprinted in the red halo surface brightness profiles at some level, and there is no compelling evidence for such features at the current time.

5.5. Subdwarf detectability as a function of distance

The luminosity functions of Digby et al. (2003) and Gould et al. (1998) have for simplicity been adopted throughout volumes A and B for all subdwarfs in the luminosity range $7.5 \lesssim M_V \lesssim 12.4$. In reality, the luminosity function is not sampled equally well at all distances, since the faintest (i.e. least massive) subdwarfs typically cannot be detected out to as large distances as the brightest ones. In fact, $M_V \approx 12.4$ stars are detected only out to a distance of order 5 kpc from the Sun in volume B, i.e. substantially smaller than the 40 kpc adopted for its outer boundary. The constraints imposed by these volumes may therefore be too strict for red halo populations composed almost entirely of the subdwarfs at the lowest masses. However, even if we completely disregard all constraints based on volume B, thereby restricting ourselves to very small distances from the Sun (≤ 2.8 kpc), we are still left with reasonably strong constraints imposed by volume A (as depicted in Fig. 3a). All $\alpha = 4.50$ populations with $\beta_{\text{red}} \geq 2.75$ are constrained to contribute less than $10^{10} M_{\odot}$ to the baryon budget for all μ_i normalizations considered. Shallower density profiles $\beta_{\text{red}} < 2.75$ do allow red halo masses in excess of $10^{10} M_{\odot}$, but these

would be in poor agreement with the values derived by Z04.

5.6. Halo smoothness

One way of sidestepping the Milky Way star counts would be to assume that the red halo stars are not smoothly distributed, but clustered. Scenarios of this type have been carefully investigated by Kerins (1997a,b), and remain a viable way of hiding the red halo population from detection in the Milky Way. The volumes A and B in which the star counts have assumed to be valid (Fig. 1), are crude representations of the actual volumes probed. In reality, the subdwarf samples used in the studies by Gould et al. (1998) and Digby et al. (2003) have been obtained in a limited number of fields, which would more accurately be represented by a large number of narrow cones probing the volume. If red halo stars were clustered, we may have missed them simply because they have so far happened to fall between the cones.

Such clusters of low-mass stars in the Milky Way halo might already be detectable as faint, extended objects in a wide-angle survey such as the SDSS (provided that a sufficient number of such clusters is located at sufficiently small distances from us), or in external galaxies, using a combination of surface photometry and star counts.

As an example, consider a star cluster of mass $4 \times 10^4 M_{\odot}$ (the mass favoured by Kerins 1997a,b) with $Z = 0.004$ and IMF slope $\alpha = 4.50$ (i.e. the values favoured by Zackrisson et al. 2006). The cluster would have an absolute magnitude of $M_I \approx -3.3$ in the Cousins *I*-band, which is ≈ 0.5 mag below the tip of the red giant branch (RGB) in a 10 Gyr old population. Objects this bright are readily detectable with the HST at distances out to at least ≈ 10 Mpc. However, objects of this type could possibly – depending on their compactness and exact distance – be mistaken for single stars when observed in the commonly used *V* and *I* filters alone, since the *V* – *I* colour of such a population is predicted to be $V - I \approx 1.7$ (assuming $\tau = 1$ Gyr and an age of 10 Gyr), similar to that of RGB stars. Multicolour data should nonetheless be able to reveal their exotic nature, since the spectra of integrated stellar populations typically differ substantially from those of individual stars.

The idea of red halo star clusters at these luminosities is very interesting in the light of recent work by Yan et al. (2008), who in the halo of the nearby galaxy M60 (distance ≈ 16 Mpc) may have detected a population of halo objects with luminosities of giants, but *izJHK* colours that are difficult to reconcile with current models of such stars. Yan et al. argue that these objects, whatever their nature, may be responsible for the anomalous colours of red halos. It remains to be investigated, however, whether the colours of these objects may be consistent with the expectations for star clusters with bottom-heavy IMFs.

5.7. The typicality of the Milky Way

Since the analysis by Z04 does not directly reveal what the variance of halo properties within the stacked sample is, we do not know what fraction of the stacked galaxies have a red halo. Perhaps some do not, and the Milky Way is just one such case. If so, we are confronted with

red halos possibly contributing significantly to the baryonic mass in some disk galaxies – but not in others. In disks at least, the baryonic Tully-Fisher relation (i.e. the relation between the total inferred stellar and gas masses vs. the rotational velocity) can be tuned via the stellar population mass-to-light ratio to show very small scatter (McGaugh et al. 2000; McGaugh 2005), which has been used as an argument that most of the baryons of disk galaxies have already been identified. Having considerable baryonic reservoirs in red halos for some disk galaxies, but not for others, would supposedly increase the scatter, but the magnitude of this effect is unclear. Moreover, there are observational indications that the Milky Way may be offset from the baryonic Tully-Fisher relation (Flynn et al. 2006). If this is the case, constraints based on the Milky Way may not be able to say anything definitive on the red halo masses of disk galaxies in general.

6. SUMMARY

By comparing the photometric properties of the red halo detected in stacked SDSS data by Z04 to the available subdwarf star counts in the Milky Way halo, we have tested the viability of models that aim to explain

the colours of red halos as due to stellar populations with abnormally high fractions of low-mass stars. We find, that a smooth halo with a bottom-heavy IMF and structural parameters similar to those of the stacked halo is completely ruled out in the Milky Way by current star count data. A halo component with a bottom-heavy IMF would have to have an overall scaling or density profile that differs substantially from that of the stacked halo to remain viable. Moreover, all permitted smooth red halo models with a density slope even remotely similar to that of the stacked halo contain far too little mass to have any bearing on the missing-baryon problem in the Milky Way. These conclusions could possibly be avoided if the red halo stars are locked up in small star clusters. We argue that such scenarios can be tested through combined star counts and deep surface photometry of the halos of nearby galaxies.

EZ acknowledges research grants from the Academy of Finland, the Swedish Research Council and the Swedish Royal Academy of Sciences. The anonymous referee is thanked for useful comments which helped improve the quality of the paper.

REFERENCES

- Alcock, C., et al. 2000, *ApJ*, 542, 281
 Belokurov, V., Evans, N. W., & Le Du, Y. 2004, *MNRAS* 352, 233
 Bell, E. F., Zucker, D. B., Belokurov, V., et al. 2008, *ApJ*, 680, 295
 Bergvall, N., & Östlin, G. 2002, *A&A*, 390, 891
 Bergvall, N., Marquart, T., Persson, C., Zackrisson, E., & Östlin, G. 2005, in *Multiwavelength Mapping of Galaxy Formation and Evolution*, ed. A. Renzini, & R. Bender, (Berlin: Springer-Verlag), p.355
 Brandner, W. 2005, in *Astrophysics and Space Science Library Volume 327, The Initial Mass Function 50 years later*, ed. E. Corbelli, F. Palte, & H. Zinnecker (Dordrecht: Springer), p.101
 Bregman, J. N. 2007, *ARA&A*, 45, 221
 Calchi Novati, S., et al. 2005, *A&A*, 443, 911
 Calchi Novati, S., de Luca, F., Jetzer, Ph., Mancini, L., & Scarpetta, G. 2008, *A&A*, 480 723
 Carollo, D., et al. 2007, *Nature*, 450, 1020
 Casagrande, L., Flynn, C., & Bessel, M., 2008, *MNRAS*, in press (preprint: arXiv0806.2471)
 Cen, R., & Ostriker, J. P. 1999, *ApJ*, 514, 1
 Chabrier, G. 2003, *PASP*, 115, 763
 Crain, R. A., Eke, V. R., Frenk, C. S., Jenkins, A., McCarthy, I. G., Navarro, J. F., & Pearce, F. R. 2007, *MNRAS*, 377, 41
 Davé, R., et al. 2001, *ApJ*, 552, 473
 de Jong, J. T. A., et al. 2006, *A&A*, 446, 855
 de Jong, R. S. 2008, *MNRAS*, 388, 1521
 Digby, A. P., Hambly, N. C., Cooke, J. A., Reid, I. N., & Cannon, R. D. 2003, *MNRAS*, 344, 583
 Fioc, M., & Rocca-Volmerange, B. 1999, preprint (astro-ph/9912179)
 Flynn, C., Holmberg, J., Portinari, L., Fuchs, B., & Jahreiß, H. 2006, *MNRAS*, 372, 1149
 Freese, K., 2000, *Physics Reports*, 333, 183
 Fukugita, M. 2004, in *International Astronomical Union Symposium no. 220*, ed. S. D. Ryder, D. J. Pisano, M. A. Walker, & K. C. Freeman (San Francisco: Astronomical Society of the Pacific) p.227
 Fukugita, M., & Peebles, P. J. E. 2004, *ApJ*, 616, 643
 Fukugita, M., & Peebles, P. J. E. 2006, *ApJ*, 639, 590
 Gardner, E., Innanen, K. A., & Flynn, C. 2008, to appear in *The Galactic Disk in Cosmological Context*, International Astronomical Union Symposium no. 254, ed. J. Andersen, J. Bland-Hawthorn, & B. Nordström (preprint: arXiv0808.0498)
 Gould, A., Flynn, C., & Bahcall, J. N. 1998, *ApJ*, 503, 798
 Gould, A. 2003, *ApJ*, 583, 765
 Gouliermis, D., Brandner, W., & Henning, T., 2006, *ApJ*, 641, 838
 Griest, K. 1991, *ApJ*, 366, 412
 Hoversten, E. A., & Glazebrook, K. 2008, *ApJ*, 675, 163
 James, P. A., & Casali, M. M. 1998, *MNRAS*, 301, 280
 Juric, M., Ivezić, Z., Brooks, A., et al. 2008 *ApJ*, 673, 864
 Kerins, E. J. 1997a, *A&A* 322, 709
 Kerins, E. J. 1997b, *A&A* 328, 5
 Klypin, A., Zhao, H., & Somerville, R. S. 2002, *ApJ*, 573, 597
 Komatsu E., et al. 2008, *ApJS*, submitted (preprint: arXiv0803.0547)
 Lequeux, J., Fort, B., Dantel-Fort, M., Cuillandre, J.-C., & Mellier, Y. 1996, *A&A*, 312, L1
 Maller, A. H., & Bullock, J. S. 2004, *MNRAS*, 355, 694
 Marigo, P., Girardi, L., Bressan, A., & Groenewegen, M. A. T., Silva, L., Granato G. L. 2007, *A&A*, submitted (preprint arXiv:0711.4922)
 Martínez-Delgado, D., Penarrubia, J., Gabany, R. J., Trujillo, I., Majewski, S. R., & Pohlen, M. 2008, *ApJ*, submitted (preprint: arXiv0805.1137)
 Massey, P. 2002, *ApJS*, 141, 81
 McGaugh, S. S., Schombert, J. M., Bothun, G. D., & de Blok, W. J. G. 2000, *ApJ*, 533, L99
 McGaugh, S. S. 2005, *ApJ*, 632, 859
 Michard, R. 2002, *A&A*, 384, 763
 Molinari, E., Buzzoni, A., Chincarini, G., & Pedrana, M.D. 1994, *A&A* 292, 54
 Nicastrro, F., et al. 2005, *Nature* 433, 495L
 Pfenniger, D., Combes, F., & Martinet, L. 1994, *A&A* 285, 79
 Pfenniger, D., & Combes, F. 1994, *A&A* 285, 94
 Prochaska, J. X., & Tumlinson, J. 2008, to appear in *Astrophysics in the Next Decade: JWST and Concurrent Facilities*, ed. X. Tielens (preprint: arXiv:0805.4635)
 Riffeser, A., Seitz, S., & Bender, R. 2008, *ApJ*, in press (preprint: arXiv0805.0137)
 Rudy, R. J., Woodward, C. E., Hodge, T., Fairfield, S. W., & Harker, D. 1997, *Nature*, 387, 159
 Sackett, P. D., Morrison, H. L., Harding, P., & Boroson, T. A. 1994, *Nature*, 370, 441
 Shang, Z., et al. 1998, *ApJ*, 504, 23
 Sirianni, M., et al. 2005, *PASP*, 117, 1049
 Sommer-Larsen, J., & Dolgov, A. 2001, *ApJ*, 551, 608
 Sommer-Larsen, J. 2006, *ApJ*, 644, 1
 Tamm, A., Tempel, E., & Tenjes, P. 2007, preprint (arXiv:0707.4375)
 Tisserand, P., et al. 2007, *A&A*, 469, 387
 van Dokkum, P. G. 2008, *ApJ*, 674, 29
 Yan, H., Hathi, N. P., & Windhorst, R. A. 2008, *ApJ*, 675, 136

- Zackrisson, E., Bergvall, N., Östlin, G., Micheva, G., & Leksell, M. 2006, *ApJ*, 650, 812
- Zackrisson, E., Bergvall, N., Flynn, C., Östlin, G., Micheva, G., & Caldwell, B. 2007, in *International Astronomical Union Symposium no. 244*, ed. J. I. Davies, & M. J. Disney, p.17
- Zackrisson, E., & Riehm, T. 2007, *A&A* 475, 453
- Zepf, S. E., Liu, M. C., Marleau, F. R., Sackett, P. D., & Graham, J. R. 2000, *AJ*, 119, 1701
- Zheng, Z., et al. 1999, *AJ*, 117, 2757
- Zibetti, S., White, S. D. M., & Brinkmann, J. 2004, *MNRAS*, 347, 556 (Z04)
- Zibetti, S., & Ferguson, A. M. N. 2004, *MNRAS*, 352, 6